ADVANCED MODELING OF UAV DYNAMICS USING ARTIFICIAL NEURAL NETWORKS AND THE OUTPUT ERROR METHOD

Pedro JIMENEZ-SOLER*, Piotr LICHOTA*, Piotr FELISIAK**

*Faculty of Power and Aeronautical Engineering, Institute of Aeronautics and Applied Mechanics, Warsaw University of Technology, Nowowiejska St. 24, 00-665 Warsaw, Poland
**Faculty of Mechanical and Power Engineering, Department of Cryogenics and Aerospace Engineering, Wrocław University of Science and Technology, Wybrzeże Wyspiańskiego 27, 50-370 Wrocław, Poland

pedro.jimenez_soler.dokt@pw.edu.pl, piotr.lichota@pw.edu.pl, piotr.felisiak@pwr.edu.pl

received 28 March 2025, revised 16 November 2025, accepted 27 November 2025

Abstract: This study presents an advanced approach to modeling Unmanned Aerial Vehicle (UAV) dynamics by integrating Artificial Neural Networks (ANNs) and the Output Error Method (OEM). Moreover, the research analyzes the longitudinal flight characteristics of the Multiplex FunCub R/C, using data from designed flight tests complemented by simulations incorporating sensor noise and drift effects. Furthermore, the study captures a comprehensive range of aerodynamic responses essential for precise system identification by employing a multistep elevator input signal. In addition, the OEM approach, a traditional parameter estimation method, offers robust statistical estimation by minimizing the discrepancies between measured and predicted outputs. However, due to the nonlinear complexities inherent in UAV flight dynamics, the study also explores ANNs, leveraging their capability to model intricate nonlinear behaviors without requiring predefined aerodynamic parameters. Subsequently, the performance of both methodologies is critically evaluated against measured aerodynamic coefficients, revealing ANNs' superior adaptability in accurately predicting complex aerodynamic interactions compared to OEM. Consequently, results indicate notable reductions in relative error, particularly in challenging aerodynamic coefficients. Overall, this research not only highlights the comparative advantages of ANNs in UAV system identification but also lays an initial structure for future advancements in UAV modeling and control systems.

Key words: Unmanned Aerial Vehicles (UAVs), Output Error Method (OEM), Artificial Neural Networks (ANNs), Maximum Likelihood Estimation (MLE), Machine Learning, System Identification, Aerodynamics, Flight Mechanics

1. INTRODUCTION

Unmanned Aerial Vehicles (UAVs) are crucial in various sectors, including aerial surveillance, environmental monitoring, precision agriculture, and disaster management [1–3]. These platforms navigate through complex environments, where stability and precise navigation are important [4–6]. Robust control systems are essential to ensure operational safety and efficiency across varied environmental and operational contexts [1,7]. At the core of these systems lies the process of system identification, which models the dynamic behaviors from observed data [8–10]. This modeling is crucial for enabling accurate predictions of UAV responses to command inputs under diverse flight conditions, thereby ensuring the effectiveness and reliability of their missions [11,12]. This study focuses on the R/C airplane Multiplex-FunCub [13], selected for its stability and payload capacity, which make it ideal for research applications [14] and utilizes a comprehensive dataset from flight tests complemented by simulations tailored for sensor noise and drift effects, providing a realistic representation of UAV dynamics. These tests are meticulously designed to extract a wide spectrum of aerodynamic responses by employing a multistep input elevator signal in the longitudinal axis. This approach determines key aerodynamic characteristics and enhances the precision of the system identification process. Building upon this robust dataset, system identification becomes crucial for translating observed behavior into predictive models.

In system identification, two widely recognized methods are Maximum Likelihood Estimation (MLE) and the Output Error Method (OEM) [8,10,15,16]. MLE is a statistical approach that identifies model parameters by selecting the values that make the observed flight data most probable. In contrast, OEM is more error-focused, aiming to minimize the gap between measured outputs—such as pitch angle or velocity—and the corresponding outputs predicted by the model. Despite their long-standing use and proven effectiveness in many scenarios, both methods frequently encounter difficulties in adequately representing the complex, nonlinear behaviors characteristic of UAV flight [17,18].

In response to these challenges, this paper advocates for integrating Artificial Neural Networks (ANNs) with experimental UAV datasets. Renowned for their ability as universal approximators, ANNs excel at capturing nonlinear relationships through highly interconnected layers and at generalizing from extensive datasets [19,20]. This capacity can substantially enhance model accuracy and robustness, especially under diverse operating conditions, offering notable improvements over traditional techniques in predicting aerodynamic characteristics [21,22]. The application of ANNs in this context demonstrates their potential to refine system identification processes and underscores their transformative impact on developing more reliable and efficient UAV control systems. The insights derived from this study are expected to contribute significantly to the field of UAV dynamics, providing a foundation for future innovations in UAV development.

The subsequent sections are organized in the following way: Section 2 presents the Dynamic Model, outlining the fundamental equations that govern UAV longitudinal motion. Section 3 discusses the Simulation setup and Flight Test, describing how flight data and simulation results are obtained, including details on the data excitation approach and the Marchand Method. Section 4 explains the Methods used for system identification, detailing the integration of MLE-based OEM and Artificial Neural Networks. Section 5 covers the Results and Discussion, comparing the performance of the identified models and highlighting key findings. Finally, Section 6 offers the Conclusion, summarizing the study's major insights and suggesting future directions for UAV dynamic modeling and control.

2. DYNAMIC MODEL

The R/C airplane model as depicted in Fig. 1, is selected for its versatility in carrying various sensors and payloads, making it an excellent choice for UAV system identification experiments.

Operating at lower speeds and lighter weight, it mirrors many UAVs commonly used in research and real-world tasks. This setup provides a controlled yet realistic platform for analyzing sensor noise impacts and validating different methods [24].

Fig. 1. Multiplex FunCub Airplane [23]

Accurate system identification for UAVs heavily depends on the underlying fidelity of their dynamic models [6]. In this study, particular attention is given to the airplane's longitudinal flight characteristics [5].This aircraft has a mass of 1.96 kg and a pitch axis moment of inertia of 0.095 kg·m². Additionally, a mean aerodynamic chord measuring 0.226m and a wing area of 0.313m². During typical flights, it cruises at around 21 m/s. Before initiating simulations, initial conditions including airspeed, pitch angle, pitch rate, and angle of attack are established based on data from typical flight tests. Aerodynamic forces and moments are subsequently computed at each step, utilizing these current states.[8]. This process yields time histories of various flight parameters, to which realistic noise levels are introduced, reflecting the performance limits of sensors.

2.1. Longitudinal Dynamics

Longitudinal motion is pivotal to predicting the aircraft's behavior under various conditions. This component of flight can be represented by a series of state equations that detail how the airspeed V, pitch angle θ, pitch rate q, and angle of attack α evolve over time [5,6,8]. These equations stem from basic flight dynamics principles and include aerodynamic forces and control inputs (elevator deflection or engine thrust).

Although this study focuses on longitudinal dynamics and treats lateral-directional effects as decoupled, the same approach could extend to lateral-directional modeling [8].

Equations 1 - 4 capture the continuous-time dynamics, incorporating factors like aerodynamic coefficients, control deflections, and external forces.

$$\dot{V} = -\frac{\bar{q}S}{m}C_D + g\sin(\alpha-\theta) + \frac{F_e}{m}cos(\alpha+\sigma_T) \quad (1)$$

$$\dot{\alpha} = -\frac{\bar{q}S}{mV}C_L + q + \frac{g}{V}cos(\alpha-\theta) - \frac{F_e}{mV}sin(\alpha+\sigma_T) \quad (2)$$

$$\dot{\theta} = q \quad (3)$$

$$\dot{q} = \frac{\bar{q}S\bar{c}}{I_y}C_m + \frac{F_e}{I_y}(l_{tx}\,sin\,\sigma_T + l_{tz}\,cos\,\sigma_T) \quad (4)$$

In these formulas, the coefficients for drag C_L, lift C_D, and pitching moment C_m are modeled as follows:

$$C_L = C_{L0} + C_{LV}\frac{V}{V_0} + C_{L\alpha}\alpha \quad (5)$$

$$C_D = C_{D0} + C_{DV}\frac{V}{V_0} + C_{D\alpha}\alpha \quad (6)$$

$$C_m = C_{m0} + C_{mV}\frac{V}{V_0} + C_{m\alpha}\alpha + C_{mq}\frac{q\bar{c}}{2V_0} + C_{m\delta_e}\delta_e \quad (7)$$

Here, $\dot{V}, \dot{\alpha}, \dot{\theta}, \dot{q}$ denote rates of parameters. The term $\bar{q}$ is dynamic pressure, while m, S, and I_y represent aircraft mass, wing area, and pitch-axis moment of inertia. Coefficients C_D, C_L, and C_m vary with V, α, and q, and depend on baseline velocity V_0 and elevator deflection δ_e.

Additional parameters encompass gravitational acceleration g, engine thrust F_e, and thrust line offsets (σ_T, l_{tx}, l_{tz}), which define the thrust line orientation and its offset from the center of gravity. Throughout both simulations and flight tests, a constant thrust is used to maintain a steady cruising speed of 21 m/s, ensuring consistency in the flight conditions.

Initially, non-dimensional aerodynamic coefficients are calculated using XFLR5, a computational software engineered for evaluating airfoils, wings, and whole aircraft at low Reynolds numbers.[25]. Through panel methods and vortex lattice models, it estimates both aerodynamic coefficients and performance metrics [26].

The output from XFLR5 serves as an initial parameter set for system identification, acting as a baseline from which real-flight behaviors can be refined [7]. Aerodynamic non-dimensional coefficients estimated from simulated data using XFLR5 software are detailed in Table 1.

Tab. 1. Aerodynamic non-dimensional coefficients

ID	Par.	Value	ID	Par.	Vale	ID	Par.	Value
1	CD_0	0.0177	5	CL_V	-0.0025	9	Cm_α	-1.6173
2	CD_V	0.0136	6	CL_α	4.2305	10	Cm_q	-8.0193
3	CD_α	0.1223	7	Cm_0	0.0446	11	$Cm_{\delta e}$	-1.4830
4	CL_0	0.1518	8	Cm_V	-0.0092			

3. FLIGHT TEST

In this study, a multi-stage process begins with data collection and analysis. The UAV is prepared for a series of flight tests and, to strengthen the overall dataset, these measurements are supplemented by simulated data as described previously. Together, these

sources yield a robust foundation for subsequent examination. This initial setup is crucial for gathering precise data that feeds into the subsequent phases of the study.

Following data collection, the process transitions into the Data Preparation phase. During this stage, the collected data is cleaned and normalized to ensure its quality and reliability, which is essential for accurate modeling [10]. The refined data then moves into the Model Development and Implementation phase, where data is employed to construct models capable of accurately identifying UAV dynamics [8].

To facilitate data collection, a 2^k experimental design is used. This method allows for the simultaneous measurement of multiple variables and their interactions, thus providing essential information with minimal testing—a benefit under operational constraints [27–29]. In this setup, three key factors are selected due to their potential influence on flight performance: external air temperature, atmospheric pressure, and wind speed. With $k = 3$ eight total tests are conducted to develop the dataset for system identification models. Flight tests were conducted at *Lotnisko Modelarskie Zalesie*, a short runway located approximately 20 km east of Warsaw, Poland, under near-zero-wind conditions, as shown in Figure 2.

Figure 3 illustrates how each test flight is systematically conducted to capture UAV's aerodynamic responses. These flights involve executing a carefully designed 3-2-1-1 elevator input sequence [8,20]. Each test begins with a manual takeoff, where the UAV climbs to a predefined altitude. Following the climb, the UAV reaches cruise altitude. During the cruise phase, the 3-2-1-1 multistep input signal is deployed by the elevator. This sequence starts with a significant deflection to sharply increase the pitch angle, followed by a moderated deflection to slightly reduce the pitch, allowing observations of the UAV's damping and stability characteristics.

For robust system identification, input signals must sufficiently excite all relevant flight modes to capture the full range of an aircraft's dynamic responses [30]. Prior research has highlighted the significance of multistep elevator inputs for analyzing longitudinal motion [31,32]. Incorporating frequencies above and below the natural frequency of the short-period mode is essential, since eigenfrequencies are subject to uncertainty and can vary with flight conditions. One effective way to achieve this coverage is by designing a series of evenly spaced pulse inputs that collectively produce a diverse power spectrum [8].

The construction of these multistep inputs involves two main steps: initially, identifying the range of frequencies required for precise aerodynamic parameter estimation; second, creating a signal that spans these frequencies [33,34]. To identify the critical frequencies, researchers often rely on Bode diagrams, which reveal how different terms in the force and moment equations respond to various input frequencies. The approach developed by Marchand [35] uses a linearized longitudinal model to illustrate how individual aerodynamic derivatives can be recognized when their frequency response surpasses roughly 10% of the maximum term [8].

Figure 4 provides an example Bode plot based on coefficients from Table 1, indicating that the 0.1–10 rad/s range generally includes both short-period and phugoid modes.

The significant frequency is chosen as $f_c = 0.468$ rad/s, and the input time interval Δt is selected so that this critical frequency is either centered or lies near the upper portion of the signal's spectrum [8]. The final 60-second elevator deflection sequence, with 1 degree amplitude and $\Delta t = 0.641$s, successfully excites both short-period and phugoid responses within the targeted frequency range.

Furthermore, the CubePilot autopilot system [36] was integrated with Mission Planner [37] software to automate the creation and execution of multistep elevator inputs. By configuring a dedicated flight model within Mission Planner, the UAV could consistently perform the required step sequences—the 3-2-1-1 input—during flight tests. This setup minimized pilot workload, ensured repeatable control deflections, and enhanced the overall reliability of the data collection process.

Fig. 2. Flight Test in an R/C Model Runway

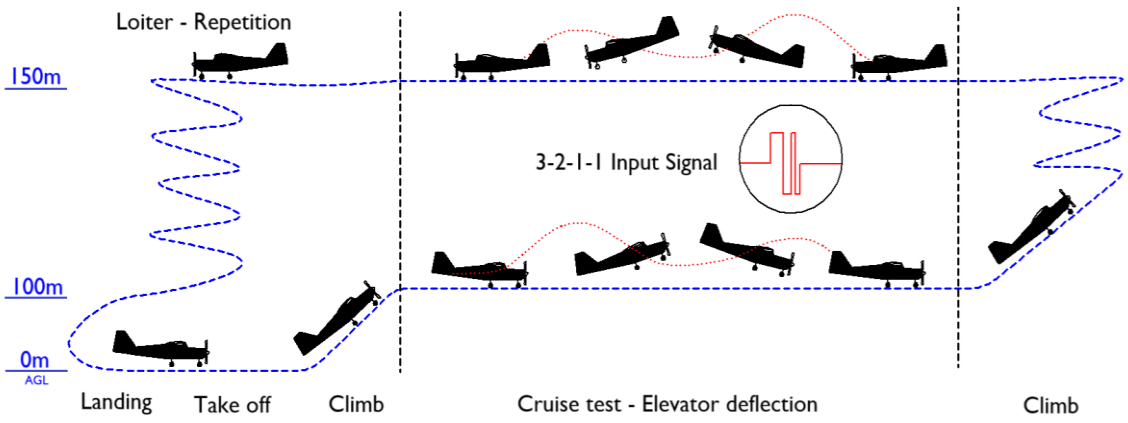

Fig. 3. Flight Envelope for Tests Performed

DOI 10.2478/ama-2025-0076

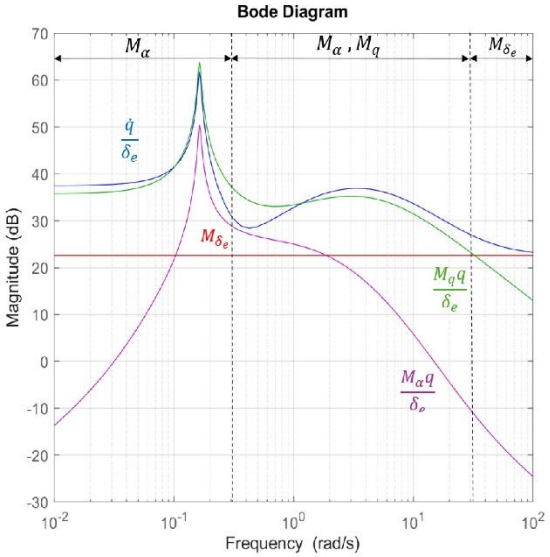

Fig. 4. Bode magnitude plot of the pitching moment for optimum frequency range determination

3.1. Data Requirements Analysis and Data Preparation

This phase focuses on the collection and preparation of flight data, involving measurement and estimation of parameters during flight tests. These parameters, categorized as channels include elevator deflection (δ_e, rad), dynamic pressure ($\bar{q}$, Pa), thrust (T, N), airspeed (V, m/s), angle of attack (α, rad), pitch attitude (θ, rad), pitch rate (q, rad/s), pitch Acceleration ($\dot{q}$, rad/s²), and longitudinal acceleration at center of gravity (a_x, m/s²). As the input signals are executed, the UAV's onboard sensors within the CubePilot autopilot system [36] capture parameters. The CubePilot features a high-performance processor and triple-redundant IMU sensors, enabling precise data.

Data preparation is executed beginning with the initial extraction of telemetry data from the autopilot logs of selected test flights. These flights are specifically chosen for their near-windless conditions and optimal elevator deflection behavior, ensuring the capture of the most reliable data for analysis.

To ensure analytical uniformity, the data is further subjected to a filtering process and resampled using interpolation to standardize the sampling frequency across all sensors to 50Hz, corresponding to a time step Δt of 0.02 seconds over a total duration of 60 seconds. This frequency is chosen as optimal for system identification [38], this resampling is critical for synchronizing the data from various sensors, as shown in Fig. 5.

It is very important to highlight that despite advancements in computational modeling, significant challenges remain that can affect the deployment and effectiveness of UAV systems [7,39,40]. A major issue is the dependency on large, representative datasets that accurately capture the UAV's operational conditions, which are often difficult to obtain due to logistical and regulatory constraints on extensive flight testing [10]. Moreover, these models need to not only accurately predict dynamics but also be computationally efficient to operate in real-time within the limited processing capabilities of UAV systems [41]. Recent studies are increasingly advocating for the use of machine learning and artificial neural networks in UAV system identification, as these advanced methods excel at handling the complexities inherent in UAV systems by learning from extensive datasets [21,22].

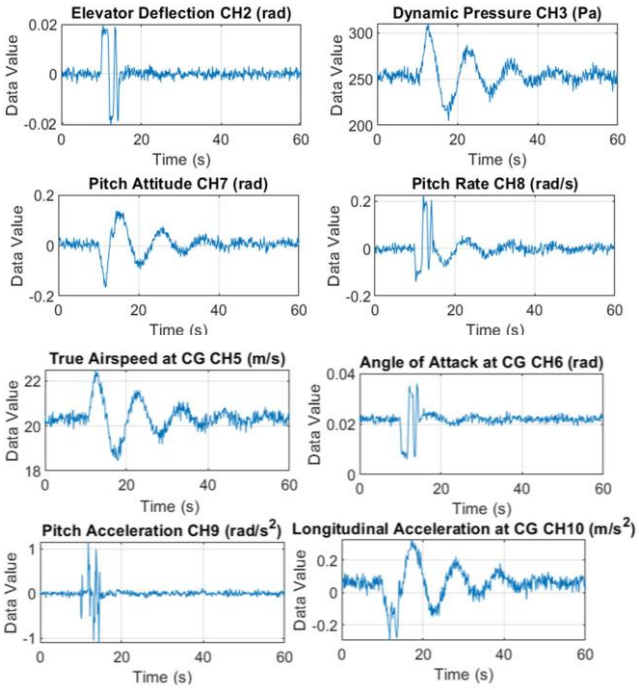

Fig. 5. Longitudinal response dataset

4. SYSTEM IDENTIFICATION METHODS

System identification for UAVs can be approached from two complementary perspectives. On the one hand, the Output Error Method (OEM), enhanced through Maximum Likelihood Estimation (MLE), offers a time-domain framework that refines model parameters by minimizing discrepancies between measured and predicted outputs under statistical assumptions. On the other hand, Artificial Neural Networks (ANNs) provide a data-centric, "black box" solution that learns complex, nonlinear input-output relationships directly from flight data—thereby reducing the reliance on a priori aerodynamic coefficients. The following subsections introduce these methods in detail, outlining their theoretical basis and practical benefits for UAV dynamics modeling.

4.1. Output Error Method (OEM) Enhanced by Maximum Likelihood Estimation (MLE)

The Output Error Method (OEM) is a time-domain approach commonly used in flight vehicle system identification. Its primary goal is to refine a model's parameters so that the gap between measured outputs and the model's predicted outputs is minimized. In practice, one begins with a set of measured outputs $y(t)$ —for instance, pitch angle or velocity—recorded during a flight test. Next, a mathematical model, which depends on an unknown parameter set θ, generates predicted outputs $\hat{y}(t, \theta)$ based on the same input commands and conditions observed during flight test. By applying the measured control deflections over time and iterating through different parameter values, the model generates a time-history of predicted states—such as pitch angle or velocity—that can be directly compared to real flight observations [8,16,42]. Figure 6 summarizes inputs and outputs in each part of the method.

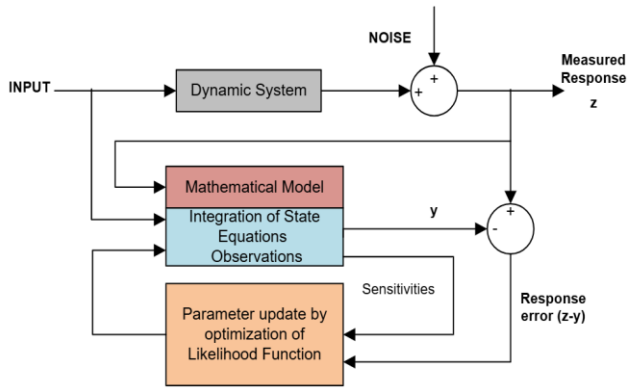

Fig. 6. Schematic of Output Error Method [8]

By comparing $y(t)$ and $\hat{y}(t,\theta)$, the output error is defined in Eq. (8):

$$e(t) = y(t) - \hat{y}(t,\theta) \tag{8}$$

By continuously refining the parameters θ, OEM attempts to make $e(t)$ as small as possible. This is typically done by summing the squared errors at each time step, as shown in Eq. 9, and employing an optimization algorithm (such as Gauss-Newton or Levenberg–Marquardt) to minimize$J(\theta)$.

$$J(\theta) = \sum_{t=1}^{T}[y(t) - \hat{y}(t,\theta)]^2 \tag{9}$$

The advantage of this approach is that it considers the entire time history of the system's response, capturing how different states (pitch angle, velocity, etc.) evolve and interact from one moment to the next [8].

Furthermore, Maximum Likelihood Estimation (MLE) is a statistical method for selecting the parameter values that are most likely to produce the observed data [8]. When incorporated into the OEM, the approach assumes that the errors $e(t)$ follow a normal (Gaussian) distribution. Under this assumption, the goal is to determine the parameter set Θ that maximizes the probability of observing the collected data.

Mathematically, this involves multiplying the likelihoods for each data point:

$$p(z|\Theta) = p(z_1|\Theta)\cdot p(z_2|\Theta)\cdots p(z_N|\Theta) = \prod_{k=1}^{N} p(z_k|\Theta) \tag{10}$$

where z_k is the measured output at a time step k. Additionally, the errors are assumed to be independent, meaning:

$$E[v(t_k)^T v(t_l)] = R\delta_{kl} \tag{11}$$

where, $\delta_{kl} = 1$ for $k = \ell$ implies that the variance of the error at time t_k is given by the diagonal elements of R, and $\delta_{kl} = 0$ for $k \neq \ell$ indicates that there is no covariance between errors at different times. This setup results in the likelihood function being a product of individual Gaussian distributions for each time point, each with mean zero and variance specified by *R*. The expression for this likelihood function, considering the independence and Gaussian assumptions, is given in Eq. 10. Therefore, Eq. 11 expresses this likelihood function in a condensed form, which is used in the optimization process to find the parameter vector Θ that minimizes the negative log-likelihood, thus maximizing the likelihood of observing the given data under the model assumptions [8]. By modeling measurement errors at each time instant as independent Gaussian random variables, this framework effectively treats sensor noise or modeling inaccuracies as unique events that do not propagate to other time steps. In practical scenarios, this assumption often aligns with the fact that external disturbances (such as sensor noise, turbulence, or small changes in flight conditions) are uncorrelated across individual measurements. Consequently, each data point contributes a separate likelihood term, and combining them as a product yields a clear, statistically robust path to estimating the parameter vector Θ.

This assumption enables the formulation of the likelihood function for an n-dimensional measurement vector across N discrete time points, utilizing a specified parameter vector Θ and a designated measurement error covariance matrix R, as detailed in Eq. 12:

$$L(z|\Theta,R) = \frac{1}{2}\sum_{k=1}^{N}[z(t_k) - y(t_k)]^T R^{-1}[z(t_k) - y(t_k)] + \frac{N}{2}\ln\big(\det(R)\big) + \frac{Nn_y}{2}\ln(2\pi) \tag{12}$$

The optimization aims to find the parameter set Θ that minimizes the negative log-likelihood, as specified in Eq. 13:

$$\widehat{\Theta}_{ML} = arg\left\{\min_{\Theta} \ln p(z|\Theta)\right\} \tag{13}$$

The process employs the Gauss-Newton method, described in Eq. 14, to ensure efficient convergence:

$$\theta_{n+1} = \theta_n - [J''(\theta_n)]^{-1}J'(\theta_n) \tag{14}$$

Hence, MLE with OEM parameters are refined within a time-domain and probabilistic framework. This interaction—sometimes called only the Output Error Method—is especially advantageous in UAV dynamics, where nonlinearities and uncertainties can be significant. The combined approach yields a robust parameter estimation procedure capable of accommodating complex aerodynamic behaviors while still providing a statistically meaningful interpretation of model–data discrepancies.

4.2. Artificial Neural Networks (ANNs)

ANNs embody a methodology for system identification, particularly adept at handling the nonlinear dynamics inherent in UAV systems. These networks differ markedly from traditional linear models in their capacity to learn complex behaviors from extensive datasets [43–45].

Artificial Neural Networks (ANNs) provide a data-centric approach to modeling UAV flight dynamics without needing explicit aerodynamic equations or *a priori* parameter estimates, as XFLR5 data that was previously described. This "black box" philosophy allows the network to learn underlying relationships directly from input-output data rather than relying on an initial guess of aerodynamic coefficients. Using the experimental-simulated data set of elevator deflection, pitch angle, velocity, and other sensor data the ANN can discern the complex mapping from these inputs to the aircraft's actual response. In contrast, a traditional model might require carefully chosen initial values for aerodynamic derivatives, which can be potentially inaccurate or difficult to obtain, especially under varied flight conditions. Instead, an ANN recognizes patterns by processing the data through interconnected layers of artificial neurons, each layer typically containing nonlinear activation functions [43–45]. Consequently, even if the exact form of the aerodynamic forces and moments remains unknown, the network can approximate the function that governs the UAV's behavior, as shown in Figure 7.

DOI 10.2478/ama-2025-0076

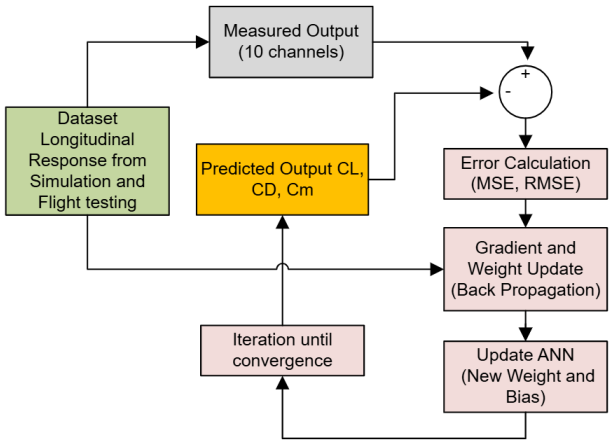

Fig. 7. Schematic of Neural Network Training for Aerodynamic Coefficient Prediction

A typical setup begins with an input layer accepting measured variables such as elevator deflection, pitch angle, or velocity; the signals then propagate through one or more hidden layers, capturing subtle interactions that may elude conventional linear models [21]. Figure 8 illustrates the schematic of a single neuron. In the final output layer, the network produces predictions such as aerodynamic coefficients or states of motion, all without needing a predefined analytical description of the aircraft. This capacity to learn from data alone makes ANNs highly suitable for UAV scenarios where flight conditions, vehicle configurations, or sensor accuracy may vary, ensuring that the system identification process remains robust and adaptable over time.

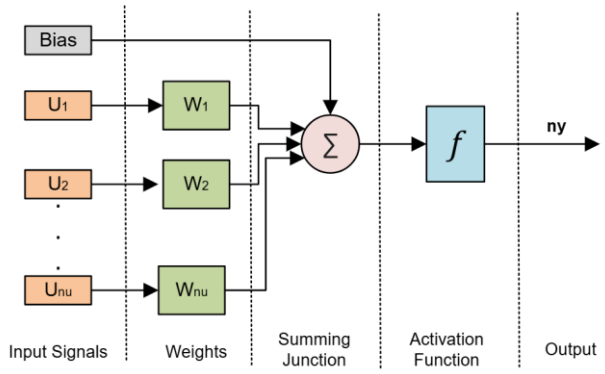

Fig. 8. Schematic of a single Neuron in ANNs

The relationship between neurons is determined by weights that adjust during the training phase to optimize network performance, governed by Eq. (15):

$$y = f(W \cdot x + b) \tag{15}$$

Where x denotes the neuron's input vector, W represents a matrix of weights, b is a bias term, and $f(\cdot)$ is the activation function. ANN training proceeds through forward propagation, where the measured input passes through the network to generate an output $\hat{y}_i$. A loss function, often the mean squared error (MSE), then quantifies the discrepancy between $\hat{y}_i$ and the measured output y_i as stated in Eq 16.

$$L = \frac{1}{n}\sum_{i=1}^{n}(y_i - \hat{y}_i)^2 \tag{16}$$

Where n is the total number of observations. Minimizing L involves backpropagation, which calculates the influence of each weight and bias on the observed error, followed by a gradient-based optimization algorithm such as gradient descent that updates the parameters:

$$W_{\text{new}} = W_{\text{old}} - \alpha \nabla_W L\,, \tag{17}$$

$$b_{\text{new}} = b_{\text{old}}\, \alpha \nabla_b L \tag{18}$$

Equations (17) and (18), illustrate how the learning rate α determines the step size for each gradient descent update of the weights and biases. A larger α can accelerate training but risks overshooting minima, whereas a smaller α typically produces more stable, albeit slower, convergence. In addition to adjusting the learning rate α, the selection of the number of hidden layers and the number of neurons within each layer is important for optimizing network performance and preventing overfitting. Employing regularization techniques, including dropout and weight decay, further boosts the model's capacity to generalize effectively across varied data scenarios by reducing the likelihood of the network memorizing the training data.

Thanks to this adaptive capability, ANNs prove especially advantageous for UAV system identification, where complex aerodynamic effects, uncertain sensor behavior, and rapidly changing flight conditions demand models capable of capturing intricate, nonlinear dynamics [17]. As they learn relationships directly from data, neural networks provide an additional layer of flexibility and resilience compared to more conventional linear models, ultimately enhancing both the accuracy and robustness of UAV dynamic modeling.

5. MODELS' DEVELOPMENT AND IMPLEMENTATION

The model development and implementation for system identification started with the integration of the OEM and Maximum Likelihood parameter estimation. This combination effectively handles noisy measurements and ensures robust parameter estimation. The initial setup involved defining a global time step variable (dt), to synchronize the numerical integration process throughout the simulation, ensuring consistency in the temporal aspects of the model the following initial conditions were set:

$$x_0 = [V_0, \alpha_0, \theta_0,] = [20.26, 0.022, 0.0089, -0.0022] \tag{19}$$

For numerical integration, various orders of the Runge-Kutta method are utilized, influencing the accuracy and stability of the simulations. At the core of the system identification process is an iterative optimization loop where system parameters are refined by minimizing a cost function. After seven iterations, convergence is achieved on parameter estimation.

Figure 9 shows measured and estimated data; the red line shows the system identified, while the blue line represents the input data. The subsequent section will discuss specific values, errors, and standard deviations.

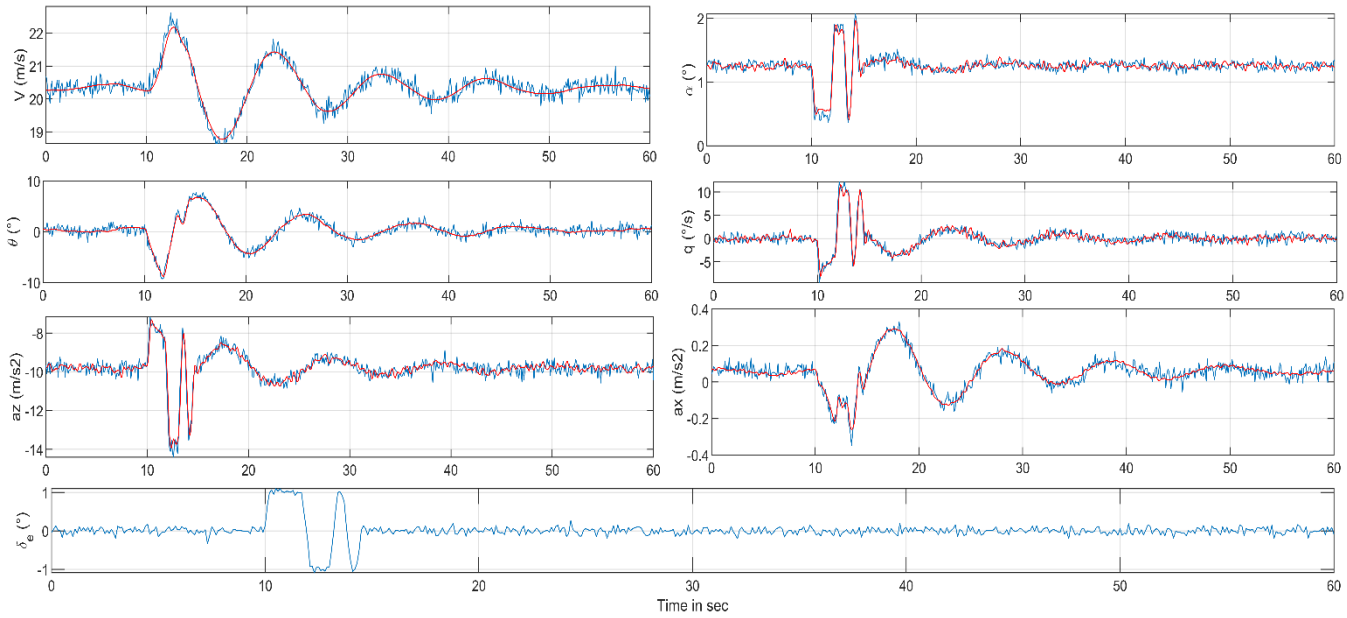

Fig. 9. Time histories of measured (blue line) and estimated parameters (red line), using OEM method

The study advances by modeling the ANNs, specifically utilizing Feed-Forward Neural Networks (FFNNs) for system identification. These networks, recommended by numerous researchers [21,46,47]. FFNNs are specifically utilized due to their proficiency in environments where only input-output relationships are observable and internal system dynamics remain unknown.

The system's architecture is deliberately designed with a streamlined, unidirectional data flow that progresses through multiple layers from input to output, without recursive connections, because it facilitates precise simulation of the causal relationships between elevator deflection and flight states, significantly enhancing the accuracy with which the resulting aerodynamic forces and moments are calculated. By avoiding recursive connections, the model avoids the complexities of feedback loops, thereby simplifying the learning process and increasing the model's output reliability as they pertain directly to UAV dynamics.

The training of the FFNNs is conducted using a backpropagation algorithm that fine-tunes weights in response to discrepancies between the predictions and the actual data, facilitating precise learning. Additionally, the FFNNs are enhanced with variants of Kalman gain, which are integrated to increase the efficiency and accuracy of the learning process. [8]. Also, hyperparameter tuning is utilized to refine the network's training process, involving adjustments to critical parameters such as the learning rate, the number of hidden layers and neurons, batch size, and training cycles.

In addition, a specialized function is used to address potential biases in measured angular rates and accelerations to correct scale factors in angles of attack. This function also calculates essential aerodynamic coefficients, providing a comprehensive understanding of the UAV's aerodynamics based on corrected flight data. The FFNNs are trained using preprocessed flight data, with the desired outputs being aerodynamic forces and moments. Initial weights are assigned randomly, which hinders the ability to precisely replicate results. However, multiple trials consistently produced a comparable level of model quality, demonstrating consistent alignment between measured data and predicted responses.[8].

The training's effectiveness is continuously monitored by tracking reductions in the loss function, reflecting the increasing accuracy of the network in modeling UAV dynamics. When setting up the neural network, fine-tuning several parameters is crucial to optimizing the learning process.

In the FFNN designed for aerodynamic modeling, the network architecture comprises three layers: an input layer, a single hidden layer, and an output layer. This hidden layer is equipped with six neurons, selected through a hyperparameter tuning process. This process involved experimental adjustments based on heuristic approaches [8,46,47], specifically using the square root of the sum of the neurons in the input and output layers to establish the optimal number of neurons.

Scaling was not applied to the input data prior to feeding it into the network, to preserve the original measurement scales. The activation function used was the Rectified Linear Unit (ReLU), which was chosen for its efficiency in handling non-linear data without introducing negative values, thus maintaining the integrity of the non-linear relationships within the aerodynamic data being modeled. The FFNN's training was characterized by repeated data processing cycles, output computation, and weight adjustment. This regimen was maintained across 2000 iterations to meet the standards of similar studies [8,17], ensuring consistency and reliability.

A key aspect of this phase was employing a modified backpropagation algorithm enhanced with Kalman gain, which played an important role in refining the learning process. Finally, the computation of total aerodynamic coefficients used the derivatives as outlined in Table 1, computed according to the equations specified from Eq. 5 to 7. As a result, Fig. 10 shows time histories between measured and estimated data of Aerodynamic Lift Coefficient C_L, Drag Coefficient C_D and C_m moment coefficient as estimated parameters of the prediction cycle.

DOI 10.2478/ama-2025-0076

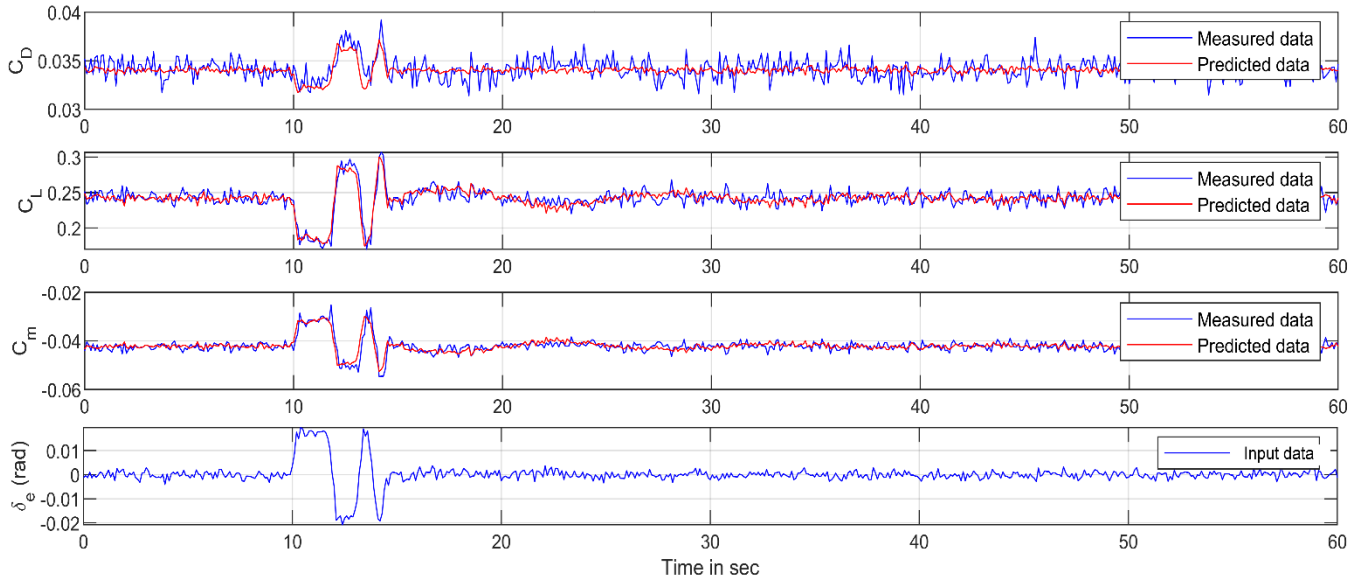

Fig. 10. Time History of Estimated parameters: ANNs Prediction Cycle

6. RESULTS AND MODELS EVALUATION

The evaluation of system identification techniques underscored the effectiveness of both the OEM and ANNs methods, with their performance detailed in Table 2, Fig. 9 and Fig.10.

The OEM method showcased robust results, particularly for the zero-lift lift coefficient (CL_0) and the lift coefficient due to the angle of attack (CL_α). These results highlight the precision of the OEM approach in modeling aerodynamic forces accurately.

In contrast, the lift coefficient due to velocity (CL_V) under the OEM method exhibited a significant relative error of 40.80%, reflecting potential uncertainties in modeling. Meanwhile, the ANNs method demonstrated a notable improvement in managing this parameter, reducing the relative error to 24%.

The ANN approach significantly improved the estimation accuracy for the parameter Cm_q , reducing the relative error from -13.07% (OEM) to 1.20%. Additionally, the ANN achieved a slight improvement in the estimation of $Cm_{\delta e}$, lowering its relative error to 0.61%. These improvements indicate that ANNs are effective in modeling dynamic behaviors, surpassing the traditional OEM in capturing certain aerodynamic characteristics.

Moreover, to further validate the data presented in Fig. 10, the coefficients C_L, C_D and C_m were evaluated using parameters estimated from OEM.

The comparison between the OEM and ANNs for aerodynamic coefficients C_L, C_D and C_m, as shown in Fig. 11, highlights varied deviation patterns throughout the evaluation.

The drag coefficient C_D error remains tightly narrowed, peaking just above 0.002, which indicates a consistent performance in drag estimation by both methods. The lift coefficient C_L error consistently stays close to zero with occasional spikes up to 0.04. Therefore, lift is accurately estimated even amid the complexities of aerodynamic modeling.

Conversely, the pitching moment coefficient C_m shows wider error fluctuations up to about 0.01, revealing more pronounced discrepancies and suggesting that C_m estimation may be more sensitive to the modeling techniques used, reflecting potential challenges in capturing dynamic aerodynamic behaviors accurately.

Tab. 2. Aerodynamic non-dimensional coefficients comparison

ID	Parameter	Estimated value OEM	Relative error OEM	Estimated value ANNs	Relative error ANNs
1	CD_0	0.0176	0.62%	0.018	0.56%
2	CD_V	0.0131	4.04%	0.013	2.94%
3	CD_α	0.1217	0.50%	0.123	0.25%
4	CL_0	0.1524	0.42%	0.153	0.46%
5	CL_V	-0.0035	40.80%	-0.003	24.00%
6	CL_α	4.2509	0.48%	4.233	0.05%
7	Cm_0	0.0443	0.61%	0.045	1.12%
8	Cm_V	-0.0095	2.83%	-0.010	10.87%
9	Cm_α	-1.5681	3.04%	-1.619	0.09%
10	Cm_q	-6.9714	13.07%	-7.923	1.20%
11	$Cm_{\delta e}$	-1.4163	4.50%	-1.492	0.61%

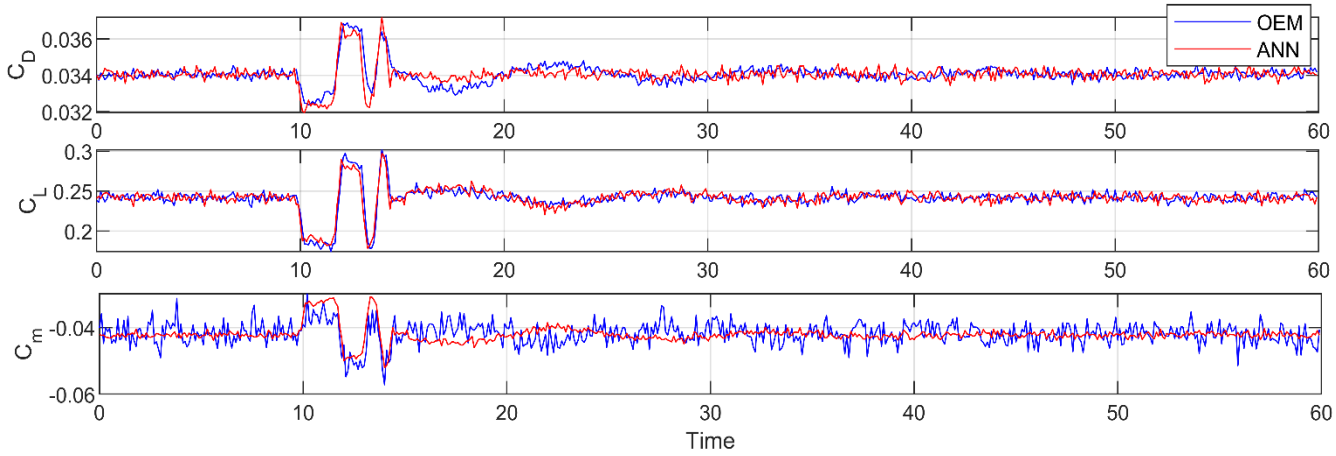

Fig. 11. Comparison of C_L, C_D and C_m between OEM and ANN

7. CONCLUSION

This study successfully used the Output Error Method (OEM), Maximum Likelihood Estimation (MLE), and Artificial Neural Networks (ANNs) to analyze the longitudinal dynamics of the Multiplex FunCub UAV. Through the application of the Gauss-Newton method, the OEM/MLE technique provided highly accurate parameter estimates, as demonstrated by the precise calculation of the drag coefficient with remarkably low relative errors. Concurrently, the Feed-Forward Neural Network (FFNN), refined with sophisticated optimization methods, effectively modeled the intricate relationships between control inputs and aerodynamic responses, validating its proficiency in predicting essential UAV dynamics.

Comprehensive data preprocessing and the strategic synergy of OEM/MLE with ANNs maximize the strengths of both approaches, enhancing the efficiency and accuracy of UAV system identification. This analysis demonstrated significant time and cost savings and the capability of ANNs to predict solely from experimental data, without *a priori* values.

However, the analysis identified greater sensitivity in the pitching moment coefficient, compared to Lift and Drag coefficients, indicating potential variances due to flight data quality and sensor accuracy. Addressing these challenges, methods like wavelet decomposition could further refine data preprocessing, improving the reliability of ANNs predictions and the overall accuracy of aerodynamic behavior modeling. This approach, as detailed in previous works [15,39], ensures more dependable input for system identification, enhancing the robustness of UAV dynamic models.

Finally, it is worth emphasizing that accurate system identification boosts the development of modern flight-control systems as well as the stability and control design of new aircraft. By applying ANN- and OEM-based identification techniques to small R/C aircraft, advanced aerodynamic models can still be obtained even when only inexpensive, low-cost sensors are available. Therefore, this capability is highly relevant for future fixed-wing UAV concepts, where accurate aerodynamic models are a prerequisite for designing robust, high-performance control architectures.

REFERENCES

1. Mohsan SAH, Othman NQH, Li Y, Alsharif MH, Khan MA. Unmanned aerial vehicles (UAVs): practical aspects, applications, open challenges, security issues, and future trends. Intel Serv Robotics. 2023;16:109–37. https://doi.org/10.1007/s11370-022-00452-4
2. Reddy Maddikunta PK, Hakak S, Alazab M, Bhattacharya S, Gadekallu TR, Khan WZ et al. Unmanned Aerial Vehicles in Smart Agriculture: Applications, Requirements, and Challenges. IEEE Sensors Journal. 2021;21:17608–19. https://doi.org/10.1109/JSEN.2021.3049471
3. Colomina I, Molina P. Unmanned aerial systems for photogrammetry and remote sensing: A review. ISPRS Journal of Photogrammetry and Remote Sensing. 2014;92:79–97. https://doi.org/10.1016/j.isprsjprs.2014.02.013
4. Dias JN. Flight-Test Determination of Longitudinal Stability Using System Identification. Journal of Aircraft. American Institute of Aeronautics and Astronautics; 2023;60:1659–74. https://doi.org/10.2514/1.C037252
5. Pamadi BN. Performance, Stability, Dynamics, and Control of Airplanes, Third Edition [Internet]. Reston, VA: American Institute of Aeronautics and Astronautics Inc.; 2015. https://doi.org/10.2514/4.102745
6. Cook MV. Flight Dynamics Principles: A Linear Systems Approach to Aircraft Stability and Control. Butterworth-Heinemann; 2012.
7. Simmons BM. System Identification of a Nonlinear Flight Dynamics Model for a Small, Fixed-Wing UAV [Internet]. Virginia Tech; 2018. http://hdl.handle.net/10919/95324. Accessed 5 Aug 2024
8. Jategaonkar RV. Flight Vehicle System Identification: A Time-Domain Methodology, Second Edition [Internet]. Reston, VA: American Institute of Aeronautics and Astronautics Inc.; 2015. https://doi.org/10.2514/4.102790
9. Dorobantu A, Murch A, Mettler B, Balas G. System Identification for Small, Low-Cost, Fixed-Wing Unmanned Aircraft. Journal of Aircraft. 2013;50:1117–30. https://doi.org/10.2514/1.C032065
10. Simmons BM, Gresham JL, Woolsey CA. Flight-Test System Identification Techniques and Applications for Small, Low-Cost, Fixed-Wing Aircraft. Journal of Aircraft. 2023;60:1503–21. https://doi.org/10.2514/1.C037260
11. Morelli E. Efficient Global Aerodynamic Modeling from Flight Data. 50th AIAA Aerospace Sciences Meeting including the New Horizons Forum and Aerospace Exposition [Internet]. Nashville, Tennessee: American Institute of Aeronautics and Astronautics; 2012. https://doi.org/10.2514/6.2012-1050
12. Simmons BM, McClelland HG, Woolsey CA. Nonlinear Model Identification Methodology for Small, Fixed-Wing, Unmanned Aircraft. Journal of Aircraft. 2019;56:1056–67. https://doi.org/10.2514/1.C035160
13. Multiplex. Multiplex Fun cub Manual [Internet]. hitecrcd; 2024. https://hitecrcd.com/files/FunCubManual.pdf.
14. Fuhrmann L, Biallawons O, Klare J, Panhuber R, Klenke R, Ender J. Micro-Doppler analysis and classification of UAVs at Ka band. 2017 18th International Radar Symposium (IRS) [Internet]. 2017; 1–9. https://doi.org/10.23919/IRS.2017.8008142
15. Lichota P. Wavelet Transform-Based Aircraft System Identification. Journal of Guidance, Control and Dynamics. 2023;46:350–61.

https://doi.org/10.2514/1.G006654
16. Tangirala AK. Principles of System Identification: Theory and Practice. Boca Raton: CRC Press; 2017. https://doi.org/10.1201/9781315222509
17. Harris J, Arthurs F, Henrickson JV, Valasek J. Aircraft system identification using artificial neural networks with flight test data. 2016 International Conference on Unmanned Aircraft Systems (ICUAS) [Internet]. 2016; 679–88.https://doi.org/10.1109/ICUAS.2016.7502624
18. Muliadi J, Kusumoputro B. Neural Network Control System of UAV Altitude Dynamics and Its Comparison with the PID Control System. Journal of Advanced Transportation. 2018;3823201. https://doi.org/10.1155/2018/3823201
19. Prasad V, Bequette BW. Nonlinear system identification and model reduction using artificial neural networks. Computers & Chemical Engineering. 2003;27:1741–54. https://doi.org/10.1016/S0098-1354(03)00137-6
20. Ertugrul E, Koyuncu E. Neural Network-based UAV System Identification from Sparse Flight Test Data. AIAA SCITECH 2023 Forum [Internet]. American Institute of Aeronautics and Astronautics. https://doi.org/10.2514/6.2023-1344
21. Gu W, Valavanis KP, Rutherford MJ, Rizzo A. UAV Model-based Flight Control with Artificial Neural Networks: A Survey. J Intell Robot Syst. 2020;100:1469–91. https://doi.org/10.1007/s10846-020-01227-8
22. Bagherzadeh SA. Nonlinear aircraft system identification using artificial neural networks enhanced by empirical mode decomposition. Aerospace Science and Technology. 2018;75:155–71. https://doi.org/10.1016/j.ast.2018.01.004
23. Multiplex Fun Cub model [Internet]. https://shop.multiplex-rc.de/en/rr-funcub-ng-blue-p4212/
24. Kownacki C. Self-Adaptive Asymmetrical Artificial Potential Field Approach Dedicated to the Problem of Position Tracking by Nonholonomic UAVs in Windy Enivroments. Acta Mechanica et Automatica. 2021;15:37–46. https://doi.org/10.2478/ama-2021-0006
25. XFLR5 - Browse Files at SourceForge.net [Internet]. https://sourceforge.net/projects/xflr5/files/
26. Septiyana A, Hidayat K, Rizaldi A, Ramadiansyah ML, Ramadhan RA, Suseno PAP, et al. Analysis of aerodynamic characteristics using the vortex lattice method on twin tail boom unmanned aircraft. Tangerang Selatan Indonesia. 2020;020003. https://doi.org/10.1063/5.0002337
27. Correa AA, Pere G, Tort-Martorell X. Experimentation order with good properties for 2 k factorial designs. Journal of Applied Statistics. Taylor & Francis; 2009;36:743–54. https://doi.org/10.1080/02664760802499337
28. Obias KCU, Say MFQ, Fernandez EAV, Chua AY, Sybingco E. A Study of the Interaction of Proportional-Integral- Derivative (PID) Control in a Quadcopter Unmanned Aerial Vehicle (UAV) Using Design of Experiment. 2019 IEEE 11th International Conference on Humanoid, Nanotechnology, Information Technology, Communication and Control, Environment and Management (HNICEM) [Internet]. 2019;1–4. https://doi.org/10.1109/HNICEM48295.2019.9072806
29. Jimenez P, Lichota P, Agudelo D, Rogowski K. Experimental Validation of Total Energy Control System for UAVs. Energies. 2019;13:14. https://doi.org/10.3390/en13010014
30. Deiler C. Aerodynamic Modeling, System Identification, and Analysis of Iced Aircraft Configurations. Journal of Aircraft. 2018;55:145–61. https://doi.org/10.2514/1.C034390
31. Seren C, Bommier F, Verdier L, Bucharles A, Alazard D. Optimal Experiment and Input Design for Flight Test Protocol Optimization. AIAA Atmospheric Flight Mechanics Conference and Exhibit [Internet]. Keystone. Colorado: American Institute of Aeronautics and Astronautics; 2006. https://doi.org/10.2514/6.2006-6280
32. Lichota P. Multi-Axis Inputs for Identification of a Reconfigurable Fixed-Wing UAV. Aerospace. 2020;7:113. https://doi.org/10.3390/aerospace7080113
33. Roeser MS, Fezans N. Method for designing multi-input system identification signals using a compact time-frequency representation. CEAS Aeronaut J. 2021;12:291–306. https://doi.org/10.1007/s13272-021-00499-6
34. Fezans N, Deiler C, Roeser MS. Generation of a Dataset for System Identification with VIRTTAC-Castor; 2019. https://elib.dlr.de/129105/
35. Marchand M. Untersuchung der Bestimmbarkeit der flugmechanischen Derivative des CCV-Versuchsträgers F-104 G. Brunswick. Germany: DFVLR. 1977.
36. The Cube User Manual V1.0. CubePilot [Internet]; 2022. https://docs.cubepilot.org/user-guides/autopilot/the-cube-user-manual
37. Flight Modes-Plane documentation [Internet]. https://ardupilot.org/plane/docs/flight-modes.html
38. Poy YH, Zarnack M, Henkenjohann M, Nolte U. Aerodynamic Derivatives Identification of a Fixed-Wing UAV using Flight Data. AIAA SCITECH 2024 Forum [Internet]. American Institute of Aeronautics and Astronautics. https://doi.org/10.2514/6.2024-0248
39. Jimenez-Soler P, Lichota P. Mitigating Sensor Quality Issues in UAV System Identification Through Wavelet Decomposition. Bulletin of the Polish Academy of Sciences Technical Sciences; 2024. https://doi.org/10.24425/bpasts.2024.152216
40. Gresham JL, Simmons BM, Fahmi J-MW, Woolsey CA. Remote Uncorrelated Pilot Inputs for Nonlinear Aerodynamic Model Identification from Flight Data. AIAA AVIATION 2021 FORUM [Internet]. American Institute of Aeronautics and Astronautics; 2021. https://doi.org/10.2514/6.2021-2792
41. Real-Time System Identification Using Deep Learning for Linear Processes With Application to Unmanned Aerial Vehicles | IEEE Journals & Magazine | IEEE Xplore [Internet]. https://ieeexplore.ieee.org/abstract/document/9130679.
42. Lichota P. Unstable tilt-rotor maximum likelihood wavelet-based identification from flight test data. AEAT. 2023;95:1275–85. https://doi.org/10.1108/AEAT-01-2023-0013
43. Krogh A. What are artificial neural networks? Nat Biotechnol. Nature Publishing Group. 2008;26:195–7. https://doi.org/10.1038/nbt1386
44. Walczak S. Artificial Neural Networks. Advanced Methodologies and Technologies in Artificial Intelligence, Computer Simulation, and Human-Computer Interaction [Internet]. IGI Global; 2019;40–53. https://doi.org/10.4018/978-1-5225-7368-5.ch004
45. Sun G, Wang S. A review of the artificial neural network surrogate modeling in aerodynamic design. Proceedings of the Institution of Mechanical Engineers. Part G: Journal of Aerospace Engineering. IMECHE. 2019;233:5863–72. https://doi.org/10.1177/0954410019864485
46. Liang Y, Li G, Xu M, Zhao J, Hao F, Shi H. An intelligent control method based on artificial neural network for numerical flight simulation of the basic finner projectile with pitching maneuver. Defence Technology. 2024;32:663–74. https://doi.org/10.1016/j.dt.2023.07.012
47. Halitim AM, Bouhedda M, Tchoketch-Kebir S, Rebouh S. Artificial neural network for tilt compensation in yaw estimation. Transactions of the Institute of Measurement and Control. SAGE Publications Ltd STM. 2024;46:2087–96. https://doi.org/10.1177/01423312231214832

Pedro Jimenez-Soler: https://orcid.org/0000-0002-3452-0843

Piotr Lichota: https://orcid.org/0000-0002-8866-7293

Piotr Felisiak: https://orcid.org/0000-0003-4965-6935